

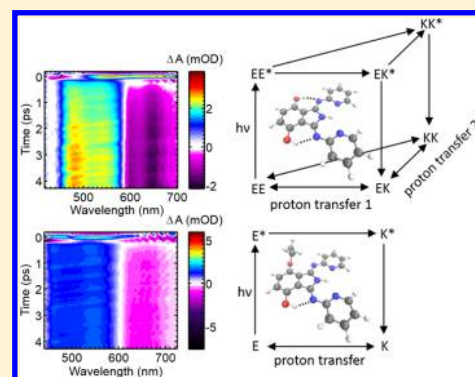
# Ultrafast Intramolecular Electron and Proton Transfer in Bis(imino)isoindole Derivatives

Eric Driscoll, Shayne Sorenson, and Jahan M. Dawlaty\*

Department of Chemistry, University of Southern California, Los Angeles, CA 90089-1062, United States

## Supporting Information

**ABSTRACT:** Concerted motion of electrons and protons in the excited state is pertinent to a wide range of chemical phenomena, including those relevant for solar-to-fuel light harvesting. The excited state dynamics of small proton-bearing molecules are expected to serve as models for better understanding such phenomena. In particular, for designing the next generation of multielectron and multiproton redox catalysts, understanding the dynamics of more than one proton in the excited state is important. Toward this goal, we have measured the ultrafast dynamics of intramolecular excited state proton transfer in a recently synthesized dye with two equivalent transferable protons. We have used a visible ultrafast pump to initiate the proton transfer in the excited state, and have probed the transient absorption of the molecule over a wide bandwidth in the visible range. The measurement shows that the signal which is characteristic of proton transfer emerges within  $\sim 710$  fs. To identify whether both protons were transferred in the excited state, we have measured the ultrafast dynamics of a related derivative, where only a single proton was available for transfer. The measured proton transfer time in that molecule was  $\sim 427$  fs. The observed dynamics in both cases were reasonably fit with single exponentials. Supported by the ultrafast observations, steady-state fluorescence, and preliminary computations of the relaxed excited states, we argue that the doubly protonated derivative most likely transfers only one of its two protons in the excited state. We have performed calculations of the frontier molecular orbitals in the Franck–Condon region. The calculations show that in both derivatives, the excitation is primarily from the HOMO to LUMO causing a large rearrangement of the electronic charge density immediately after photoexcitation. In particular, charge density is shifted away from the phenolic protons and toward the proton acceptor nitrogens. The proton transfer is hypothesized to occur both due to enhanced acidity of the phenolic proton and enhanced basicity of the nitrogen in the excited state. We hope this study can provide insight for better understanding of the general class of excited state concerted electron–proton dynamics.



## INTRODUCTION

Coupling of electron and proton motion is of central importance in a wide range of chemical phenomena, including natural and artificial light harvesting,<sup>1–6</sup> enzymatic reactions,<sup>7,8</sup> and synthetic organic chemistry.<sup>9</sup> In many proton-requiring redox reactions it is hypothesized that concerted transfer of electron and proton occurs through lower reaction barriers compared to stepwise transfer. A challenge in contemporary chemical dynamics is to measure, explain, and ultimately control such correlated motion of charges in the excited states.<sup>10,11</sup>

Photocatalytic redox reactions that are relevant for energy conversion and solar light harvesting often involve transfer of several electrons and protons. For example, photocatalytic oxidation of water requires removal of four electrons and four protons from two water molecules, making its mechanisms challenging to understand and study. To elucidate such correlated motion of electrons and protons, it is necessary to resort to simpler model systems. Photoacids<sup>12,13</sup> and molecules with excited state intramolecular proton transfer (ESIPT)<sup>14</sup> capability serve this purpose and have been known for decades.

In these systems, optical excitation, often of a conjugated electronic system, renders an attached phenolic group acidic. While in the excited state, the phenolic proton is transferred either to another molecule or to a proton acceptor within the same the molecule.<sup>15</sup> The dynamics of such processes have been extensively studied with ultrafast time-resolution both experimentally and theoretically.<sup>16–18</sup> In particular, questions such as double proton transfer,<sup>19–24</sup> involvement of intramolecular vibrational degrees of freedom,<sup>23,25–28</sup> the role of impulsively excited vibrations in transferring the proton, and the role of skeletal versus direct –OH vibrations,<sup>25,29</sup> have been debated. The origin of photoacidity is electronic charge redistribution in the excited state, which influences the motion of protons. The details of such coupling between electrons and protons remains an area of active study.<sup>12,26</sup> For example, whether the proton motion is a consequence, rather than a cause of electronic charge redistribution has been de-

Received: March 26, 2015

Revised: April 27, 2015

Published: May 1, 2015

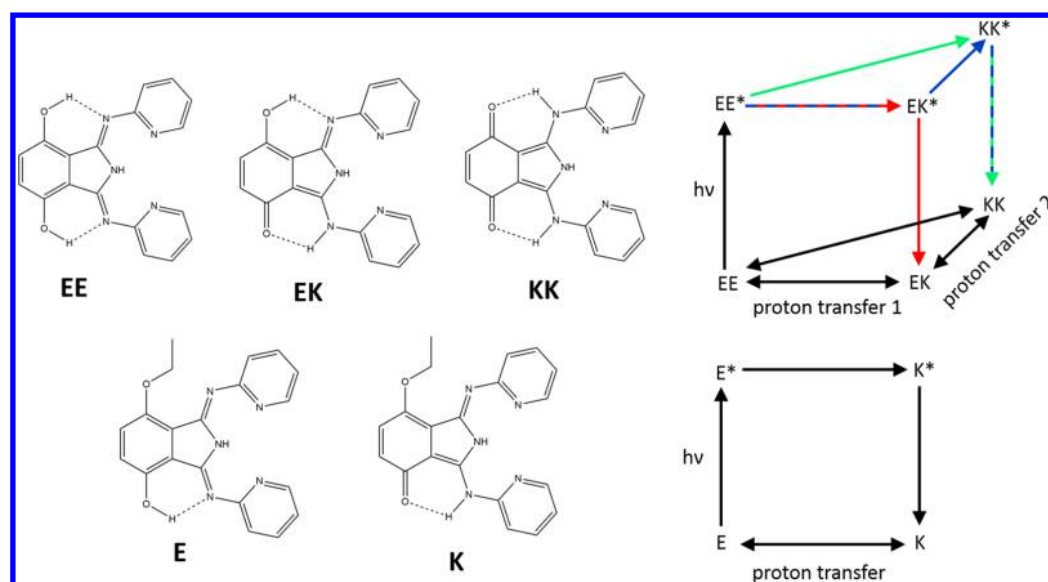


**Figure 1.** Chemical species discussed in this paper, denoted with “E” for enol and “K” for keto. (top) The three possible tautomers of the diol molecule and a schematic showing their interconversion in the ground and excited states. Three possible mechanisms for relaxation are shown in color: single proton transfer (red), stepwise double proton transfer (blue), and concerted proton transfer (green). (bottom) The two possible tautomers of the ethoxy-substituted molecule (ethoxy-ol) and their interconversion.

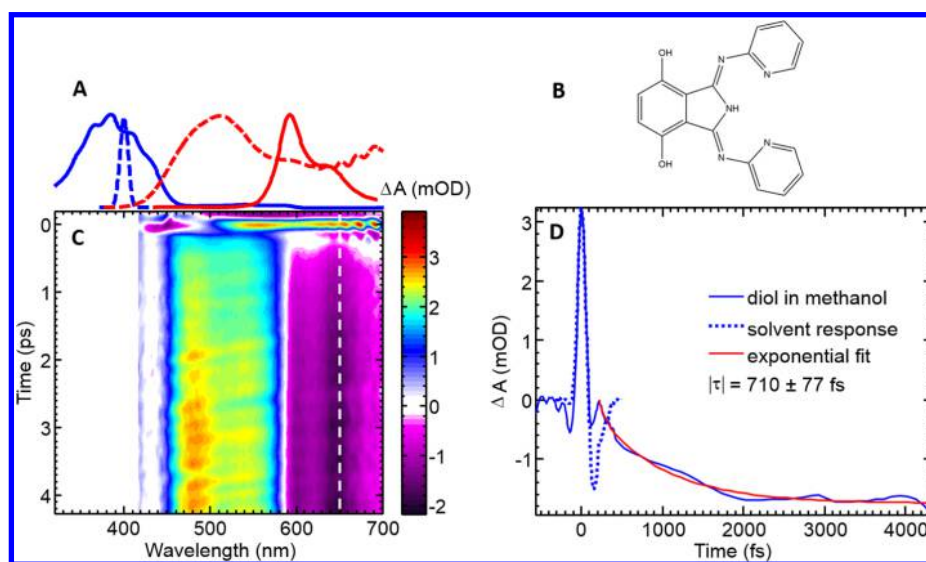


**Figure 2.** TA of the diol in methanol. (a) Steady-state absorption (blue) and emission (red) spectra of the diol in methanol. Pump (dashed blue) and probe (dashed red) pulse spectra. (b) 1,3-Bis(imino)isoindole diol, shown in the enol–enol tautomer as it exists in the electronic ground state. (c) Visible pump–white light probe TA over 4 ps. (d) A temporal slice of transient absorption along the dashed line in (c) through  $\lambda = 650$  nm. The stimulated emission shows single exponential behavior. The solvent shows some TA features at short times (dashed blue line and Figure 2 in the Supporting Information) which are not interpreted or fitted.

bated.<sup>12,29,30</sup> Apart from serving as model systems for ultrafast proton transfer, photoacids and ESIPT molecules have several applications including optical pH-jump agents,<sup>31,32</sup> laser dyes,<sup>33</sup> fluorescent probes,<sup>34</sup> molecular photoswitches,<sup>35</sup> photostabilizers, high energy radiation detectors, and white light emitting single molecules,<sup>36</sup> which are either envisaged or realized. A complete review of such systems is beyond the capacity of this introduction.

Here, we study two derivatives, shown in Figure 1, of a recently synthesized 1,3-bis(imino)isoindole motif with ESIPT capability.<sup>37</sup> A distinct feature of 1,3-bis(2-pyridylimino)-4,7-dihydroxyisoindole, which will be referred to as the “diol” derivative, is the existence of two equivalent transferable

protons. The current study of this molecule has three main goals. First, we report the measured timescale of proton transfer in the excited state using ultrafast broad-band pump–probe spectroscopy and compare the dynamics to smaller ESIPT molecules. Second, to find out whether one or both of the protons transfer in the excited state, we compare the proton transfer dynamics between the diol and 1,3-bis(2-pyridylimino)-4-ethoxy-7-hydroxyisoindole, referred to as the “ethoxy-ol”, which only has one proton available for transfer. Finally, we show computational results to correlate the intramolecular redistribution of electronic charge density with the motion of protons. We will chart out a path for further theoretical and experimental investigations, with emphasis on understanding

the coupling between electronic charge redistribution and proton motion.

## METHODS

**Materials.** The compounds 1,3-Bis(2-pyridylimino)-4,7-dihydroxyisoindole and 1,3-bis(2-pyridylimino)-4-ethoxy-7-hydroxyisoindole were prepared via the procedures in ref 37. Solutions of approximately 2 mM were prepared in methanol, dichloromethane, and hexane.

**Transient Absorption.** A pump pulse centered at 400 nm was generated by frequency, doubling the output of a 1 kHz Ti:sapphire amplifier (Coherent Legend Elite HE+) in BBO. A white light continuum probe was prepared by focusing the 800 nm Ti:sapphire output onto a 3.0 mm thick sapphire window. The probe spectrum spans the entire visible range and is shown in Figure 2A. The pump was passed through a polarizer to set its polarization to the magic angle with respect to the probe to eliminate rotational diffusion effects. The pump and probe beams were attenuated to 400  $\mu$ W and 120  $\mu$ W, respectively, with neutral density filters for sample and blank spectra. The pump beam was modulated at 500 Hz using an optical chopper (Thorlabs). The probe was spectrally resolved at a 1 kHz sampling rate using a 320 mm focal length spectrometer with 150 g/mm gratings (Horiba iHR320) and a 1340  $\times$  100 CCD array (Princeton Instruments Pixis). The focal spot size diameter for the pump (probe) was  $180 \pm 30 \mu$ m ( $150 \pm 30 \mu$ m). A cross correlation of pump and probe was done using the nonresonant response of a 0.5 mm thick sapphire plate with a large pump power, 700  $\mu$ W. The cross correlation (Figure 1 of the Supporting Information) shows that the probe pulse has a parabolic chirp, which is corrected by fitting and time shifting data after collection. Each spectral component has a non-resonant response time of about 200 fs, which is considered the instrument resolution. The samples were flowed through a fused quartz flow cell with 0.1 mm of path length.

**Computational.** Ground state geometries and molecular orbitals were calculated using B3LYP/6-31+G\* with the Q-Chem<sup>38</sup> software package. Singlet excitation energies and excited state geometries were calculated using TD-B3LYP/6-31G\*. All calculations were done in the gas phase.

## RESULTS

First we will discuss the steady-state absorption and emission of the molecule and relate it to the enol and keto forms of the compound. As in other ES IPT molecules, there is a large shift between the absorption and fluorescence bands. Absorption occurs in the enol tautomer of the molecule in the band of  $\lambda < 450$  nm. Proton transfer occurs in the excited state and results into the keto tautomer, which fluoresces in the 570–700 nm band. A weak emission centered at 420 nm is observed and attributed to enol fluorescence. Both absorption and emission wavelengths show a blue shift with respect to increasing solvent polarity. Since the shifts in absorption and emission are approximately the same energy, the Stokes shift is relatively independent of solvent (Table 1). The large Stokes shifted emission is due to the significant reorganization of the molecules in the excited state associated with the proton transfer. It should be pointed out that some degree of proton transfer is expected in the ground state as well,<sup>37</sup> as indicated by the long-wavelength tail of the absorption spectrum (Figure 2A). However, the ground state equilibrium is far shifted in

**Table 1. Experimental and Calculated Stokes Shifts for Various ES IPT Species**

compound	experimental (cm <sup>-1</sup> )		
	solvent		
	methanol	chloroform	hexane
diol	9150	9051	9139
ethoxy-ol	9240	9513	9632
emitting species	calculated (cm <sup>-1</sup> )		
	theory (TD-B3LYP)		
	LR-PCM/ TZVP <sup>a</sup>	SS-PCM/ TZVP <sup>a</sup>	gas phase/6-31G* <sup>b</sup>
KK*	7904	7017	4302
EK*	7339	5807	3657
K*	–	–	5887

<sup>a</sup>Dichloromethane PCM. See Table 4 in ref 39. <sup>b</sup>This work.

favor of the enol form for the compounds discussed in this paper.

The purpose of our transient absorption (TA) measurement is to identify the timescale of proton transfer by pumping the enol tautomer and following the spectral signatures of the keto tautomer in time. In such measurements, the signal arises from a net addition of at least three processes. Ground state bleach (GB) results from the depletion of ground state population due to the pump and contributes to the signal with a negative sign. Stimulated emission (SE) from an excited species also results in a negative signal. Excited state absorption (EA) due to a pumped species contributes with a positive sign. Fortunately, in the molecules in this study, the steady-state absorption and steady-state fluorescence bands are widely separated, thus conveniently separating GB and SE based on wavelength. Furthermore, the pump is only absorbed by the enol form, and fluorescence occurs from the keto form after proton transfer, making the interpretation of the data relatively easy. The main signature of the proton transfer will be the emergence of a negative signal due to SE in the fluorescence band. The purpose of the TA measurement is to resolve the emergence of this band after pumping.

The time-resolved spectrum of the diol in methanol is shown in Figure 2. The pump is centered near 400 nm in the absorption band, while the probe mainly spans the keto fluorescence band and the region of separation between the absorption and fluorescence. As expected, the major feature of the data is the emergence of a negative signal in the 590–700 nm band due to SE from the keto form after proton transfer. Concurrent with the negative signal, a spectrally wide positive signal with a peak near 480 nm also appears. The positive signal is assigned to EA from the keto form. Its spectral overlap with the SE signal causes the peak of the negative signal to appear red shifted with respect to the steady-state fluorescence spectrum. A separate temporal slice of the negative signal over a 0.4 nm bandwidth is shown in Figure 2D for clarity and is fit to an exponential (residual plotted in Figure 3 of the Supporting Information). The time constant of this signal,  $|\tau| = 710 \pm 77$  fs, is the time constant of proton transfer in the excited state and is one of the main findings of our work. Once again, the large separation between the absorption and fluorescence bands allows us to have almost nonoverlapping pump and probe and thus the GB signal does not contribute significantly to our measurement. This is convenient since it allows us to explain the transient spectrum at longer times only



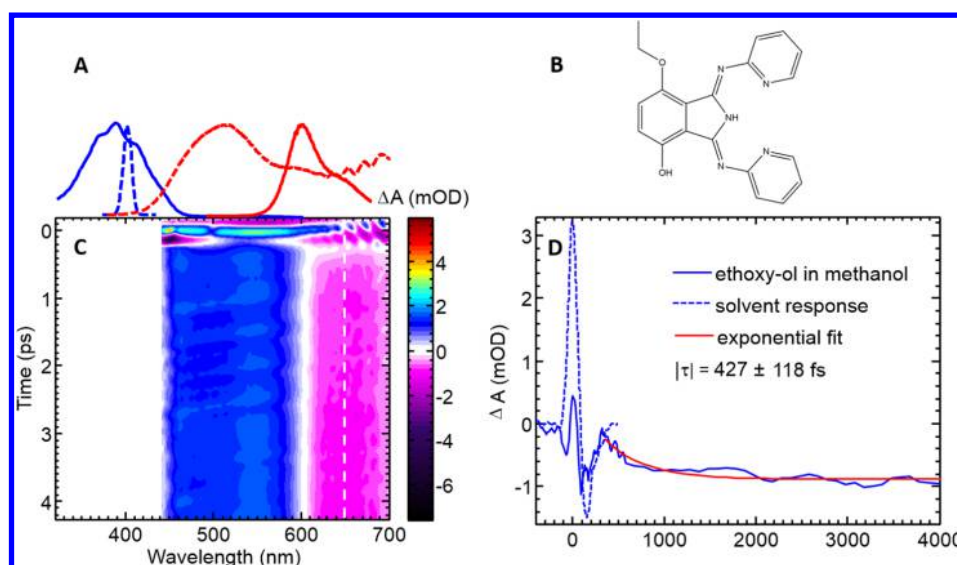


**Figure 3.** TA of the ethoxy-ol in methanol. (a) Steady state absorption (blue) and emission (red) spectra of the ethoxy-ol in methanol. Pump (dashed blue) and probe (dashed red) pulse spectra. (b) Ethoxy-substituted isoindole, shown in the enol tautomer. (c) Visible pump-white light probe TA over 4 ps. (d) A temporal slice of transient absorption along the dashed line in (c) through  $\lambda = 650$  nm.

in terms of SE and EA of the keto form. Although not directly relevant to proton transfer, a separate piece of information is gleaned from the broad nature of the positive signal and its observed maximum near 480 nm. It gives a glimpse of the second excited state  $S_2$  of the keto form. On the basis of this data,  $S_1$  can absorb photons as low energy 600 nm to access  $S_2$  and shows maximum absorption for 480 nm photons. Such a relatively clear signal for the  $S_1$  to  $S_2$  transition is made possible by the large separation between absorption and fluorescence bands which allows a clear spectral region for measuring the EA signal alone, with little interference from the competing GB and SE processes.

Transient absorption experiments in other solvents showed qualitatively similar dynamics. Fitting a single exponential to the fluorescence band in chloroform (Figure 5 of the Supporting Information) and cyclohexane (Figure 6 of the Supporting Information) found time constants of  $|\tau| = 530 \pm 14$  fs and  $|\tau| = 1.23 \pm 0.32$  ps, respectively. This variation is potentially due to the difference in solvent polarity, where a more polar solvent is expected to stabilize the charge-transferred excited state more easily and result in a faster rate. However, the observed rate in methanol does not conform to this trend and is potentially due to hydrogen bonding. As is conventional, the data at the region of pump–probe overlap is not interpreted due to several possible time-ordered interactions between the pump and the probe, as well as signal contribution from the solvent and flow cell (see Figure 2 of the Supporting Information). The pump–probe overlap is measured separately in a nonresonant medium and spans  $\sim 200$  fs (see Figure 1 of the Supporting Information).

To identify whether one or both protons get transferred in the excited state, we performed TA experiments on the ethoxy-ol derivative, which is only capable of a single proton transfer (shown in Figure 3B). As reported earlier,<sup>37</sup> the steady-state fluorescence spectrum of this compound (Figure 3A) has a fluorescence peak which is slightly red-shifted with respect to diol, but otherwise qualitatively similar. Since proton transfer in the excited state is associated with a significant geometry change, which manifests as a large Stokes shift, one may expect two proton transfers to exhibit an even larger Stokes shift

compared to a single proton transfer. A similar conclusion is indeed supported by a recent TD-DFT calculation.<sup>39</sup> On the basis of this, a natural conclusion would be to expect a much larger Stokes shift for the diol, if the diol did transfer both protons. However, experimental fluorescence spectra show that the diol molecule has a slightly smaller Stokes shift compared to the ethoxy-ol. Table 1 compares the predicted Stokes shifts from ref 39 for single and double proton transfer in the diol to the experimentally observed Stokes shifts in the diol and the ethoxy-ol forms. Thus, the similarity between the fluorescence spectra of the diol and ethoxy-ol molecules is considered partial evidence that only one of the two protons in the diol molecule transfers in the excited state. With transient absorption spectroscopy, we wanted to find out if there are differences in dynamics between the two molecules.

The TA data for the ethoxy-ol is shown in Figure 3 and exhibits qualitative similarities to the diol: a negative signal in the fluorescence band and a positive EA signal at shorter wavelengths. Fitting of the transient at 650 nm, returned a time constant of  $427 \pm 118$  fs.

## DISCUSSION

The cause of proton transfer in the excited state is electronic charge redistribution. Thus, to identify the mechanism of the transfer, it is necessary to look at the spatial extent of the HOMO and LUMO and the nature of charge redistribution induced by light. Our purpose here is a qualitative description of the phenomena in the excited state, with emphasis on gaining insight, rather than an exact simulation of the process. We encourage further theoretical investigations on this front. TD-DFT has proved to be a useful method for predicting spectroscopic properties of ESIPT compounds.<sup>40–43</sup> The electronic structure of the diol has been studied previously,<sup>39</sup> using TD-B3LYP/TZVP in a dichloromethane ( $\epsilon = 8.93$ ) PCM and is summarized briefly below. Our purpose is to first compare the electronic structure of the diol and ethoxy-ol compounds. Second, we would like to identify the electronic structure changes upon optical excitation that lead to proton transfer.

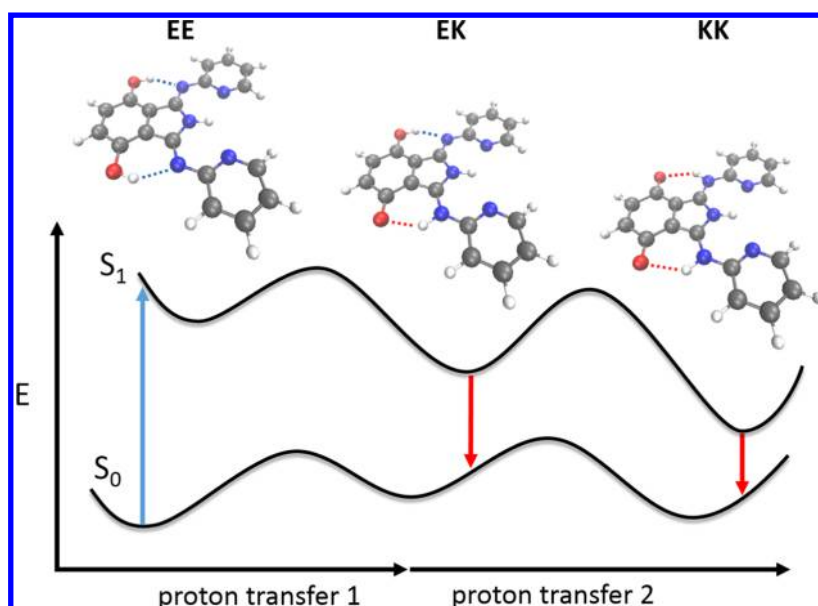


**Figure 4.** Cartoon of the diol potential energy surface resulting from stepwise proton transfer events. The blue arrow shows optical excitation of the EE tautomer, while the red arrows show possible emission from EK\* and KK\* tautomers. Although this diagram is meant to be qualitative, the spacing between levels and heights of the barriers are drawn based on calculations by Su.<sup>39</sup>

Su et al.<sup>39</sup> have calculated energy barriers to proton transfer in the ground and excited states for the diol by a relaxed potential energy surface scan. In the stepwise mechanism (Figure 4), only one N–H nuclear coordinate is scanned at a time (EE\* → EK\* → KK\*). In the concerted mechanism, both N–H coordinates are scanned symmetrically (EE\* → KK\*). In comparing the two ESIPT mechanisms, they predicted the stepwise mechanism to have, in the excited state, a barrier of 1322 cm<sup>-1</sup> for the first proton transfer and a barrier of 2685 cm<sup>-1</sup> for the second proton transfer. The concerted PES is predicted to have an excited state barrier of 4343 cm<sup>-1</sup>. Additionally, they were able to optimize the geometry of the two transition states involved in the stepwise mechanism. The concerted mechanism's transition state was not found, and in fact, the calculation would only converge to one of the two stepwise transition states. The smaller barrier to stepwise transfer as well as the optimized transition states were used to predict that the stepwise mechanism is more likely.

Using these computed potentials as guidance, we performed our own calculations to compare the excited states of the diol to the ethoxy-ol and to see if our predictions are compatible with experimental spectra. It can be seen that electronic excitation in both compounds is very similar by their almost identical absorption spectra (solid blue lines in Figures 2A and 3A). Gas phase TD-B3LYP calculations found singlet excitations at 2.97 eV (399 nm) and 3.11 eV (417 nm) in rough agreement with observed absorption maxima for the diol and ethoxy-ol, respectively. These S<sub>0</sub> → S<sub>1</sub> excitations are predicted to be composed primarily of transitions between the frontier molecular orbitals (Figure 5), for both compounds. The calculated HOMO → LUMO transitions show that electron density is expected to shift from the benzene and proton donating oxygen portion of the indole to a more delocalized configuration with increased density on the pyrrole, pyridines, and proton-accepting nitrogens.

Excited state geometry optimization done by Su et al.<sup>39</sup> on EE\* shows that optical excitation leads to a symmetric lengthening of both O–H bonds and the corresponding

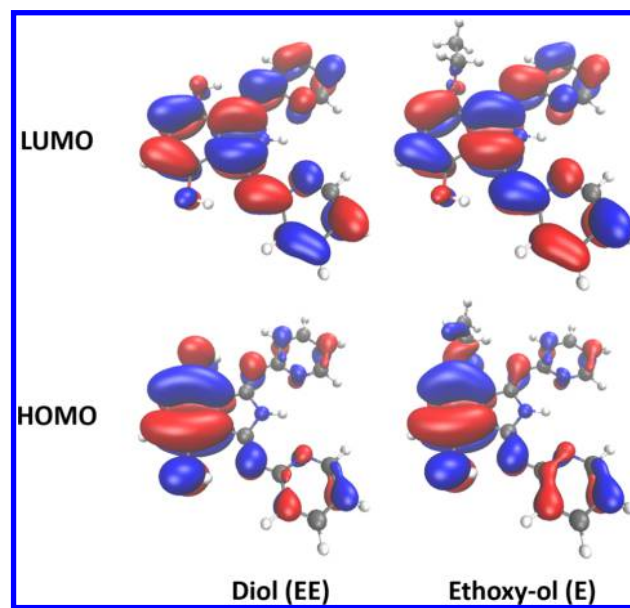


**Figure 5.** Frontier molecular orbitals of the diol and ethoxy-ol in the EE and E tautomers. TD-DFT calculations suggest that the S<sub>0</sub> → S<sub>1</sub> excitation is primarily between the HOMOs and LUMOs. Upon optical excitation electron density shifts from around the benzene and hydroxyl groups toward the pyrrole and pyridine groups in both compounds.

shortening of N–H bonds. This suggests that excitation to the Franck–Condon region places the compounds on the S<sub>1</sub> potential energy surface such that nuclear motion is induced along the proton transfer coordinates. They have concluded that two stepwise proton transfers occur in the diol, based on the calculated barrier heights in the potential energy surfaces along the proton transfer coordinates. However, one should bear in mind that upon Franck–Condon excitation a large amount of excess vibrational energy is available and distributed nonthermally among several modes. The experiment shows that vibrational relaxation in the excited state while still in the

enol form (i.e., prior to proton transfer) leads to a weak fluorescence with a Stokes shift of  $2500\text{ cm}^{-1}$ , indicating that the optical excitation of the enol form is distinctly not a  $0 \rightarrow 0$  transition. Such nonequilibrium vibrational energy can render an Arrhenius-like analysis of proton transfer less appropriate. For that reason, the utility of theoretical models should be evaluated based on their ability to explain and possibly match the experimental ultrafast measurements of proton transfer times, for example those presented in this work.

Chemical intuition would lead one to think that since a single ESIPT can result in a Stokes shift of over  $9000\text{ cm}^{-1}$ , double ESIPT would produce an even larger Stokes shift. Following along this line of reasoning, we refer to the experimentally measured Stokes shifts of the diol and the ethoxy-ol (Table 1). As mentioned earlier, the diol, which in principle can transfer two protons, has a slightly smaller Stokes shift compared to the ethoxy-ol, which can transfer only one proton. This observation gives rise to two interpretations: (1) two ESIPT processes occur in the diol and the second has either a minimal effect on the  $S_0 - S_1$  gap or increases it slightly, thereby decreasing the Stokes shift in contradiction to chemical intuition, or (2) only a single ESIPT process occurs in the diol and the observed fluorescence is from  $EK^*$ . Theoretical investigations done in a PCM<sup>39</sup> and our own gas phase calculations (Table 1) yield results in accordance with the chemically intuitive idea that the second ESIPT should increase the Stokes shift by a substantial amount. Thus, the first interpretation is not supported by theory, leaving the second interpretation as more plausible. The experimentally observed slightly larger Stokes shift of the ethoxy-ol compared to the diol is also supported by the gas phase calculations and seems to arise from the structural differences that are independent of proton transfer between the two cases. Thus, this observation reminds us that even when two equivalent protons are available for transfer, it is quite possible that only one will transfer. This important point should be taken into consideration in the analysis of all excited state multiproton processes.

Another plausible experimental measure in favor of double ESIPT would be biexponential dynamics of the emergence of the SE band (i.e., emergence of the product). However, both the ethoxy-ol and the diol exhibit dynamics that are fit reasonably well with single exponentials with  $|t| \sim 427\text{ fs}$  and  $|t| \sim 710\text{ fs}$ , respectively. This similarity in the single exponential dynamics of the diol and ethoxy-ol compounds lends more credibility to the single ESIPT mechanism in the diol. One may argue that the diol dynamics is indeed biexponential, with the first time constant too rapid ( $<100\text{ fs}$ ) for us to observe and assign within our time resolution. However, there is some reason to rule out that possibility. A single proton transfer in ethoxy-ol occurs with a time constant of  $|t| \sim 427\text{ fs}$  and is conveniently measurable in our experiment. In a possible two-proton transfer scenario in the diol, it is reasonable to argue that the first proton transfer would also occur within similar timescales and would not remain obscured due to our time-resolution. Since the observed data for the diol fits well to a single exponential, it is likely due to a single proton transfer only. Of course, a possible concerted two-proton transfer process would also give rise to a single exponential. But it can be ruled out based on other evidence, in particular, the similarity of the Stokes shifts between the diol and the ethoxy-ol, as argued in the previous paragraph.

Once again, while not directly relevant to proton transfer, comparison of the positive signal between the diol and the

ethoxy-ol forms reveals the differences in their  $S_2 - S_1$  gaps. The peak of the positive absorption for the ethoxyl-ol occurs near  $550\text{ nm}$ , in contrast to  $480\text{ nm}$  for the diol form. Although the ethoxy substitution does not seem to have strongly influenced the steady-state absorption and fluorescence, it has managed to reduce the  $S_2 - S_1$  gap significantly. The larger influence of the ethoxy substitution on the  $S_2$  surface compared to the  $S_1$  surface is an interesting auxiliary finding of this work. It may be argued that the  $S_2$  state has a larger energy and spatial extent and thus experiences the substituted ethoxy group more readily compared to the  $S_1$  state. Full explanation of this effect is outside the scope of this work.

Previous work on smaller ESIPT molecules has shown that coherent nuclear motion (i.e., wavepackets) imprint their signature on the visible TA data.<sup>23,29</sup> This phenomenon manifests as an oscillatory component in the TA which lasts for a few picoseconds. The oscillations often match in frequency to low energy ( $<500\text{ cm}^{-1}$ ) skeletal modes of the molecule that move the geometry along the proton transfer coordinate. This effect has been used to distinguish between concerted and stepwise double ESIPT mechanisms based on the symmetry of the associated normal mode for other diol-like compounds. In our data, no dominant oscillation in the TA traces are observed (see Figures 4–6 of the Supporting Information). The absence of such oscillations in the results presented here are most likely due to the larger number of atoms compared to previously studied ESIPT compounds. The larger size of the molecules gives rise to a larger vibrational density of states at low energies, with no single frequency dominating the TA signal, thus producing an effective damping of oscillations in the TA.

## CONCLUSION

Understanding the correlated motion of protons and electrons on ultrafast timescales is a contemporary challenge in chemical dynamics. The molecules studied here are model systems for understanding optically induced ultrafast proton transfer. Using broadband transient absorption spectroscopy, we have identified the time-constants of proton transfer in two derivatives, one where a single proton transfer is possible (ethoxy-ol) and one where, in principle, two proton transfers are possible (diol). On the basis of similarity in dynamics, the magnitude of the Stokes shifts, and electronic structure calculations, we conclude that a single ESIPT process in the diol is the most likely scenario. We hope that these results can be beneficial in designing chemical motifs for driving excited state redox reactions where concerted motion of several electrons and protons are involved.

## ASSOCIATED CONTENT

### Supporting Information

Further data. The Supporting Information is available free of charge on the ACS Publications website at DOI: 10.1021/acs.jpca.5b02889.

## AUTHOR INFORMATION

### Corresponding Author

\*E-mail: dawlaty@usc.edu. Tel: 213-740-9337.

### Notes

The authors declare no competing financial interest.



## ACKNOWLEDGMENTS

The authors acknowledge support from the University of Southern California start-up grant and the AFOSR YIP Award (FA9550-13-1-0128). S.S. was supported by the University of Southern California Provost Fellowship. We thank the Mark E. Thompson group at USC for providing materials, particularly Dr. Kenneth Hanson (now at Florida State University) and Dr. Peter Djurovich. We have benefited from fruitful discussions with Dr. Shirin Faraji (University of Southern California) about quantum chemistry calculations.

## REFERENCES

- (1) Bediako, D. K.; Solis, B. H.; Dogutan, D. K.; Roubelakis, M. M.; Maher, A. G.; Lee, C. H.; Chambers, M. B.; Hammes-Schiffer, S.; Nocera, D. G. Role of Pendant Proton Relays and Proton-Coupled Electron Transfer on the Hydrogen Evolution Reaction by Nickel Hangman Porphyrins. *Proc. Natl. Acad. Sci. U.S.A.* **2014**, *111*, 15001–15006.
- (2) Warren, J. J.; Mayer, J. M. Moving Protons and Electrons in Biomimetic Systems. *Biochemistry* **2015**, *54*, 1863–1878.
- (3) Cukier, R.; Nocera, D. Proton-Coupled Electron Transfer. *Annu. Rev. Phys. Chem.* **1998**, *49*, 337–369.
- (4) Mayer, J. Proton-Coupled Electron Transfer: A Reaction Chemist's View. *Annu. Rev. Phys. Chem.* **2004**, *55*, 363–390.
- (5) Huynh, M.; Meyer, T. Proton-Coupled Electron Transfer. *Chem. Rev.* **2007**, *107*, 5004–5064.
- (6) Hammes-Schiffer, S. Introduction: Proton-Coupled Electron Transfer. *Chem. Rev.* **2010**, *110*, 6937.
- (7) Reece, S.; Nocera, D. Proton-Coupled Electron Transfer in Biology: Results from Synergistic Studies in Natural and Model Systems. *Annu. Rev. Biochem.* **2009**, *78*, 673–699.
- (8) Carra, C.; Iordanova, N.; Hammes-Schiffer, S. Proton-Coupled Electron Transfer in a Model for Tyrosine Oxidation in Photosystem II. *J. Am. Chem. Soc.* **2003**, *125*, 10429–10436.
- (9) Rono, L. J.; Yayla, H. G.; Wang, D. Y.; Armstrong, M. F.; Knowles, R. R. Enantioselective Photoredox Catalysis Enabled by Proton-Coupled Electron Transfer: Development of an Asymmetric Aza-Pinacol Cyclization. *J. Am. Chem. Soc.* **2013**, *135*, 17735–17738.
- (10) Hammes-Schiffer, S. Proton-Coupled Electron Transfer: Classification Scheme and Guide to Theoretical Methods. *Energy Environ. Sci.* **2012**, *5*, 7696.
- (11) Hammes-Schiffer, S.; Stuchebrukhov, A. a. Theory of Coupled Electron and Proton Transfer Reactions. *Chem. Rev.* **2010**, *110*, 6939–6960.
- (12) Spry, D. B.; Fayer, M. D. Charge Redistribution and Photoacidity: Neutral Versus Cationic Photoacids. *J. Chem. Phys.* **2008**, *128*, 084508.
- (13) Arnaut, L. G.; Formosinho, S. J. Excited-State Proton Transfer Reactions I: Fundamentals and Intermolecular Reactions. *J. Photochem. Photobiol., A* **1993**, *75*, 1–20.
- (14) Formosinho, S. a. J.; Arnaut, L. G. Excited-State Proton Transfer Reactions II: Intramolecular Reactions. *J. Photochem. Photobiol., A* **1993**, *75*, 21–48.
- (15) Agmon, N. Elementary Steps in Excited-State Proton Transfer. *J. Phys. Chem. A* **2005**, *109*, 13–35.
- (16) Douhal, A.; Lahmani, F.; Zewail, A. H. Proton-transfer reaction dynamics. *Chem. Phys.* **1996**, *207*, 477–498.
- (17) Mohammed, O. F.; Xiao, D.; Batista, V. S.; Nibbering, E. T. J. Excited-State Intramolecular Hydrogen Transfer (ESIHT) of 1, 8-Dihydroxy-9, 10-anthraquinone (DHAQ) Characterized by Ultrafast Electronic and Vibrational Spectroscopy and Computational Modeling. *J. Phys. Chem. A* **2014**, *118*, 3090–3099.
- (18) Vendrell, O.; Moreno, M.; Lluch, J. M.; Hammes-Schiffer, S. Molecular Dynamics of Excited State Intramolecular Proton Transfer: 2-(2'-Hydroxyphenyl)-4-methylxazole in Gas Phase, Solution, and Protein Environments. *J. Phys. Chem. B* **2004**, *108*, 6616–6623.
- (19) Mordziński, A.; Grabowska, A. Intramolecular Single and Double Proton Transfer in Excited Benzoxazoles. Distinction between Concerted and Stepwise Reaction Mechanisms. *J. Mol. Struct.* **1984**, *114*, 337–341.
- (20) Mordziński, A.; Kühnle, W. Kinetics of Excited-State Proton Transfer in “Double” Benzoxazoles: 2,5-Bis(2-benzoxazolyl)-4-methoxyphenol. *J. Phys. Chem.* **1986**, *90*, 1455–58.
- (21) Takeuchi, S.; Tahara, T. The Answer to Concerted Versus Step-Wise Controversy for the Double Proton Transfer Mechanism of 7-Azaindole Dimer in Solution. *Proc. Natl. Acad. Sci. U.S.A.* **2007**, *104*, 5285–5290.
- (22) Marks, D.; Zhang, H.; Borowicz, P.; Grabowska, A.; Glasbeek, M. Femtosecond Intramolecular Proton Transfer in Photoexcited Mono- and Dienol Derivatives of Bipyridine. *Chem. Phys. Lett.* **1999**, *309*, 19–28.
- (23) Stock, K.; Schrieffer, C.; Lochbrunner, S.; Riedle, E. Reaction Path Dependent Coherent Wavepacket Dynamics in Excited State Intramolecular Double Proton Transfer. *Chem. Phys.* **2008**, *349*, 197–203.
- (24) Randino, C.; Ziólek, M.; Gelabert, R.; Organero, J. A.; Gil, M.; Moreno, M.; Lluch, J. M.; Douhal, A. Photo-Deactivation Pathways of a Double H-Bonded Photochromic Schiff Base Investigated by Combined Theoretical Calculations and Experimental Time-Resolved Studies. *Phys. Chem. Chem. Phys.* **2011**, *13*, 14960–14972.
- (25) de Vivie-Riedle, R.; de Waele, V.; Kurtz, L.; Riedle, E. Ultrafast Excited-State Proton Transfer of 2-(2'-Hydroxyphenyl)benzothiazole: Theoretical Analysis of the Skeletal Deformations and the Active Vibrational Modes. *J. Phys. Chem. A* **2003**, *107*, 10591–10599.
- (26) Lubner, S.; Adamczyk, K.; Nibbering, E. T. J.; Batista, V. S. Photoinduced Proton Coupled Electron Transfer in 2-(2'-Hydroxyphenyl)-benzothiazole. *J. Phys. Chem. A* **2013**, *117*, 5269–79.
- (27) Barbatti, M.; Aquino, A. J. a.; Lischka, H.; Schrieffer, C.; Lochbrunner, S.; Riedle, E. Ultrafast Internal Conversion Pathway and Mechanism in 2-(2'-Hydroxyphenyl)benzothiazole: A Case Study for Excited-State Intramolecular Proton Transfer Systems. *Phys. Chem. Chem. Phys.* **2009**, *11*, 1406–15.
- (28) Mohammed, O. F.; Lubner, S.; Batista, V. S.; Nibbering, E. T. J. Ultrafast Branching of Reaction Pathways in 2-(2'-Hydroxyphenyl) Benzothiazole in Polar Acetonitrile Solution. *J. Phys. Chem. A* **2011**, *115*, 7550–7558.
- (29) Schrieffer, C.; Lochbrunner, S.; Ofial, A. R.; Riedle, E. The Origin of Ultrafast Proton Transfer: Multidimensional Wave Packet Motion vs. Tunneling. *Chem. Phys. Lett.* **2011**, *503*, 61–65.
- (30) Silverman, L. N.; Spry, D. B.; Boxer, S. G.; Fayer, M. D. Charge Transfer in Photoacids Observed by Stark Spectroscopy. *J. Phys. Chem. A* **2008**, *112*, 10244–10249.
- (31) Gutman, M. The pH Jump: Probing of Macromolecules and Solutions by a Laser-Induced, Ultrashort Proton Pulse-Theory and Applications in Biochemistry. *Methods Biochem. Anal.* **1984**, *30*, 1–103.
- (32) Barooah, N.; Mohanty, J.; Pal, H.; Bhasikuttan, A. C. Cucurbituril-Induced Supramolecular pKa Shift in Fluorescent Dyes and its Prospective Applications. *Proc. Natl. Acad. Sci., India, Sect. A* **2014**, *84*, 1–17.
- (33) Piechowska, J.; Huttunen, K.; Wroble, Z.; Lemmetyinen, H.; Tkachenko, N. V.; Gryko, D. T. Excited State Intramolecular Proton Transfer in Electron-Rich and Electron-Poor Derivatives of 10-Hydroxybenzo[h]quinoline. *J. Phys. Chem. A* **2012**, *116*, 9614–20.
- (34) Wu, K.-C.; Lin, Y.-S.; Yeh, Y.-S.; Chen, C.-Y.; Ahmed, M. O.; Chou, P.-T.; Hon, Y.-S. Design and Synthesis of Intramolecular Hydrogen Bonding Systems. Their Application in Metal Cation Sensing Based on Excited-State Proton Transfer Reaction. *Tetrahedron* **2004**, *60*, 11861–11868.
- (35) Sobolewski, A. L. Reversible Molecular Switch Driven by Excited-State Hydrogen Transfer. *Phys. Chem. Chem. Phys.* **2008**, *10*, 1243–1247.
- (36) Park, S.; Ji, E. K.; Se, H. K.; Seo, J.; Chung, K.; Park, S. Y.; Jang, D. J.; Medina, B. n. M.; Gierschner, J.; Soo, Y. P. A White-Light

Emitting Molecule: Frustrated Energy Transfer Between Constituent Emitting Centers. *J. Am. Chem. Soc.* **2009**, *131*, 14043–14049.

(37) Hanson, K.; Patel, N.; Whited, M. T.; Djurovich, P. I.; Thompson, M. E. Substituted 1,3-Bis(imino)isoindole Diols: A New Class of Proton Transfer Dyes. *Org. Lett.* **2011**, *13*, 1598–1601.

(38) Krylov, A. I.; Gill, P. M. Q-Chem: An Engine for Innovation. *WIREs Comput. Mol. Sci.* **2013**, *3*, 317–326.

(39) Su, Y.; Chai, S. A TDDFT study of the excited-state intramolecular proton transfer of. *J. Photochem. Photobiol., A* **2014**, *290*, 109–115.

(40) Syetov, Y. TDDFT Calculations of Electronic Spectra of Benzoxazoles Undergoing Excited State Proton Transfer. *J. Fluoresc.* **2013**, *23*, 689–696.

(41) Jang, S.; Jin, S. I.; Park, C. R. TDDFT Potential Energy Functions for Excited State Intramolecular Proton Transfer of Salicylic Acid, 3-Aminosalicylic Acid, 5-Aminosalicylic Acid, and 5-Methoxysalicylic Acid. *Bull. Korean Chem. Soc.* **2007**, *28*, 2343–2353.

(42) Sobolewski, A. L.; Domcke, W. Ab Initio Potential-Energy Functions for Excited State Intramolecular Proton Transfer: A Comparative Study of o-Hydroxybenzaldehyde, Salicylic Acid and 7-Hydroxy-1-indanone. *Phys. Chem. Chem. Phys.* **1999**, *1*, 3065–3072.

(43) Aquino, A. J. A.; Lischka, H.; Hättig, C. Excited-state Intramolecular Proton Transfer: A Survey of TDDFT and RI-CC2 Excited-State Potential Energy Surfaces. *J. Phys. Chem. A* **2005**, *109*, 3201–3208.